Available online at www.sciencedirect.com
SCIENCE DIRECT®
Bioorganic & Medicinal Chemistry Letters 16 (2006) 228–234
Bioorganic & Medicinal Chemistry Letters

The crystal structures of 3-TAPAP in complexes with the urokinase-type plasminogen activator and picrate

Ewa Żesławska,[a] Uwe Jacob,[b] Jörg Stürzebecher[c] and Barbara J. Oleksyn[d,*]

[a]*Department of Chemistry, Pedagogical University, ul. Podchorążych 2, 30-084 Kraków, Poland*
[b]*Max-Planck-Insitut für Biochemie, Abteilung Strukturforschung, Am Klopferspitz 18A, 82152 Martinsried, Germany*
[c]*Zentrum für Vaskuläre Biologie und Medizin, Friedrich-Schiller-Universität Jena, Nordhäuser Strasse 78, 99089 Erfurt, Germany*
[d]*Faculty of Chemistry, Jagiellonian University, ul. R. Ingardena 3, 30-060 Kraków, Poland*

Received 5 January 2005; revised 11 August 2005; accepted 30 August 2005
Available online 3 October 2005

Abstract—The urokinase-type plasminogen activator (uPA) is a protein involved in tissue remodeling and other biological processes. The inhibitors of uPA have been shown to prevent the spread of metastasis and tumor growth, and accordingly this enzyme is widely accepted as a promising anticancer target. In this work, we have investigated the conformation of the uPA inhibitor 3-TAPAP in two different crystalline environments of a picrate and a uPA complex. These structures were compared to the known structure of the 3-TAPAP in the complex with trypsin. In the complexes with the proteins, trypsin, and uPA, the binding mode of 3-TAPAP is similar. A larger difference in the conformation, in the comparison to these structures, has been observed by us in the 3-TAPAP picrate crystal. This observation contradicts the hypothesis that 3-TAPAP derivatives inhibit serine proteinases in preformed stable conformations.

Plasminogen activators (PA) are serine proteinases, which activate plasminogen to plasmin. Plasmin is a broad spectrum proteinase which catalyzes the degradation of a variety of protein substrates. These substrates include fibrin,[1] fibronectin, laminin,[2] vitronectin,[3] proteoglycans,[4] and collagen.[5] With this activity, plasmin is involved in tissue remodeling, angiogenesis, embryogenesis, pathogen and tumor cell invasion, and also in metastasis.[6,7] The process of plasminogen activation in a healthy organism is strictly controlled through the availability of PAs and interaction with specific inhibitors. The human PAs exist in two forms known as tissue-type (tPA) and urokinase-type (uPA).

Both uPA and tPA are similar to each other in sequence and structure. In the active site, uPA carries the two amino acids Lys98A and Ala98A, as well as the two replacements of Tyr99 to His99 and Ser195 to Ala195. uPA and tPA appear to have different biological functions.[5,8] The main role of tPA is thought to be the dissolution of blood clots,[9] whereas uPA is involved in tissue remodeling, cellular migration, cancer invasion, and metastasis.[10–12] It has been found that uPA-catalyzed plasminogen activation is rate-limiting for tumor invasion and/or formation of distant metastasis.[13] Presence of uPA in human tumor cell environments finally caused the search for several strategies to inhibit the activity of this enzyme. Specific active site inhibitors or blocking antibodies for the specific uPA receptor effectively delay the process of tumor progression.[14,15] It has been reported that using anti-uPA antibodies could prevent tumor cell invasion, but not their metastasis to lung in mice.[16] Antisense oligodeoxynucleotides directed to uPA expression led to a reduction in uPA expression in human ovarian carcinoma cells. Furthermore, uPA antisense oligodeoxynucleotides applied to nude mice which had prior been inoculated with tumorigenic human ovarian cancer cells led to a significant reduction in tumor mass.[17] Invasion of human ovarian cells was significantly inhibited by the addition of enzymatically inactive uPA fragments.[18,19]

Synthetic inhibitors of uPA have been shown to decrease cancer growth and the rate of metastasis.[20,21] Since uPA is a trypsin-like serine proteinase, most of the described inhibitors of uPA contain groups which

Keywords: Crystal structure; Urokinase; Inhibitor; Picrate; X-ray diffraction.
* Corresponding author. Tel.: +48126632267; fax: +48126340515; e-mail: oleksyn@chemia.uj.edu.pl

0960-894X/$ - see front matter © 2005 Elsevier Ltd. All rights reserved.
doi:10.1016/j.bmcl.2005.08.089

mimic the basic side chain of arginine. One family of known uPA inhibitors contains either an amidine or a guanidine group, and the crystal structures of several of these inhibitors in complex with uPA have been extensively studied,[22–26] in search for new anticancer drugs.

In this paper, we present the crystal structures of an inhibitor containing a benzamidine group: N_α-[4-toluene sulfonyl]-D,L-*m*-amidino-phenylalanyl-piperidine (3-TAPAP) to examine the effect of different crystalline environments on its conformation. 3-TAPAP has been the lead structure for the development of large inhibitor series, whose complexes with several serine proteinases have been determined.[27] One derivative (UKI-1D)[22] has already finished the phase I of clinical trials. We describe preparation and the structure determinations of 3-TAPAP picrate, as well as the crystal structure of 3-TAPAP in complex with the catalytic domain of uPA (βc-uPA). The structural results concerning the conformation and hydrogen-bonding of 3-TAPAP in these two environments are compared to each other, as well as with the known structure of 3-TAPAP in complex with trypsin.[27]

Preparation of 3-TAPAP picrate and crystal structure determination. The N_α-[4-toluene sulfonyl]-D,L-*m*-amidino-phenylalanyl-piperidine (3-TAPAP) was obtained by the method described previously.[28] Preparation of 3-TAPAP picrate was carried out by dissolving stoichiometric amounts of 3-TAPAP hydrochloride and picric acid in hot ethanol. After cooling, an amorphous yellow salt precipitated, which after filtration was dissolved and submitted to crystallization. Crystals suitable for X-ray analysis were obtained from ethanol using a method of slow evaporation of the solvent. Within 3 weeks, dark yellow crystals appeared at 20 °C.

All diffraction data were collected using Kappa CCD diffractometer and processed with HKL Denzo and Scalepack.[29] The structure was solved by use of the SHELXS[30] program, a final refinement was performed by SHELXL97,[31] and ORTEP was used for molecular graphics.[32] The crystal data, intensity measurement, and refinement details are summarized in Table 1.

Preparation of βc-uPA–3-TAPAP complex, data collection, and structure refinement. The crystallization of Cys122Ser mutant of the serine proteinase domain of uPA (βc-uPA) in complex with benzamidine suitable for soaking experiments has been described elsewhere.[22] A crystal of this complex was soaked for one week at 4 °C in harvesting solution (0.125 M sodium citrate, pH 5.2, 1 M $(NH_4)_2SO_4$, and 1.25 M Li_2SO_4) containing a suspension of the inhibitor 3-TAPAP. This crystal was mounted in a capillary. X-ray data were collected at 16 °C using an image plate detector (Mar Research, Germany) installed on a rotating anode generator (Rigaku, Japan) operating at 50 kV and 80 mA, and evaluated with the CCP4 program package.[33] Starting coordinates were taken from the βc-uPA-benzamidine structure[22] to obtain initial difference density for the bound 3-TAPAP. A molecular model of the inhibitor was constructed with HyperChem and built into the electron density using 'O.[34] The structure was crystallographically refined using standard protocols of CNS[35] and the Engh and Huber[36] geometric restraints. Water molecules were added into the density when well-defined $F_o - F_c$ density contoured at 2.5 σ coincided with $2F_o - F_c$ density contoured at 1.0 σ. Finally, individual restrained B factors were refined, and the crystallographic weights were set to values, where the R_{free} runs through a shallow minimum. Data collection and refinement statistics are given in Table 2.

Table 1. Crystal data, intensity measurement, and refinement details for 3-TAPAP picrate

Crystal data	Data collection
$C_{22}H_{29}N_4O_3S{\cdot}C_6H_2N_3O_7{\cdot}2H_2O$	19268 measured reflections
M_r = 1315.31	5799 independent reflections
Monoclinic, *I*2/a	3705 reflections with $I > 2\sigma(I)$
a = 16.0689(1) Å	R_{int} = 0.1370
b = 18.9464(1) Å	θ_{max} = 25°
c = 21.5561(2) Å	$-19 \leqslant h \leqslant 19$
α = 90.000(0)°	$-22 \leqslant k \leqslant 22$
β = 93.276 (3)°	$-25 \leqslant l \leqslant 22$
γ = 90.000(0)°	
V = 6551.98 Å^3	Refinement
Z = 8	Refinement on F^2
D_x = 1.37 Mgm^{-3}	$R[F^2 > 2\sigma(F^2)]$ = 0.092
Mo Kα, λ = 0.71073 Å	$wR(F^2)$ = 0.249
Θ = 0.998°–25.028°	5799 reflections
μ = 0.17 mm^{-1}	509 parameters
T = 293(2) K	H-atom positions calculated
Prism	and refined as riding model
0.3 × 0.4 × 0.5 mm	$w = 1/[\sigma^2(F_o^2) + (0.0861P)^2 + 10.29P]$
	where $P = (F_o^2) + (2F_c^2)/3$
	$(\Delta/\sigma)_{mean}$ = 0.000
	$(\Delta/\sigma)_{max}$ = 0.000
	$\Delta\rho_{max}$ = 0.45 eÅ^{-3}
	$\Delta\rho_{min}$ = −0.32 eÅ^{-3}

3-TAPAP picrate. The projection of 3-TAPAP picrate with its atom numbering is given in Figure 1. The asymmetric unit consists of one molecule of the 3-TAPAP cation, a picrate anion, and disordered water molecules. The molecule of 3-TAPAP forms hydrogen bonds with picrate ions. 3-TAPAP is a big molecule containing benzamidine, 3-toluene, and piperidine groups.

The amidine group is protonated and conjugated with benzene ring, which is suggested by the bond lengths of C7-N5, C7-N4, and C7-C8, which are 1.307(5), 1.304(5), and 1.485(5) Å, respectively. In the earlier described structures of benzamidine and benzdiamidine, the amine groups are not protonated.[37,38] The bond lengths between carbon and nitrogen atoms in these structures are 1.344(3), 1.294(3) Å, and 1.349(2), 1.283(2) Å, respectively. The localization of electrons in a single and double C–N bond of the amidine group, reported in Refs. 37 and 38, is not observed in our structure. The angle between the C7-N4 and C7-N5 bonds in the amidine group of 3-TAPAP is 119.8(4)°, whereas in the benzamidine and benzdiamidine structures its values are 124.4(2)° and 119.5(1)°, respectively. The angle be-

Table 2. Crystal data, intensity measurement, and refinement details for βc-uPA–3-TAPAP

Space group $P2_12_12_1$	R_{fac} 19.6%
Cell parameters	R_{free} 23.5%
a = 53.07 Å, b = 54.80 Å, c = 82.54 Å,	
α = 90°, β = 90°, γ = 90°	
Resolution 2.0 Å	RMSD bonds 0.006 Å
Range of last resolution shell 2.0–2.1 Å	$I/\sigma(I)$: overall = 5.5, last shell = 1.9
Completeness (overall/last shell) 90.3/90.2	RMSD angles 1.20°
Multiplicity 2.4	No. of protein atoms/average B-factor 1952/25 Å^2
R_{merge} (overall) 10.7%,	
R_{merge} (for last resolution shell) 37.0%	No. of inhibitor atoms/average B-factor 30/24 Å^2
Number of unique reflections 14733	No. of solvent atoms/average B-factor 117/43 Å^2
	No. of sulfate ions/average B-factor 2/33 Å^2

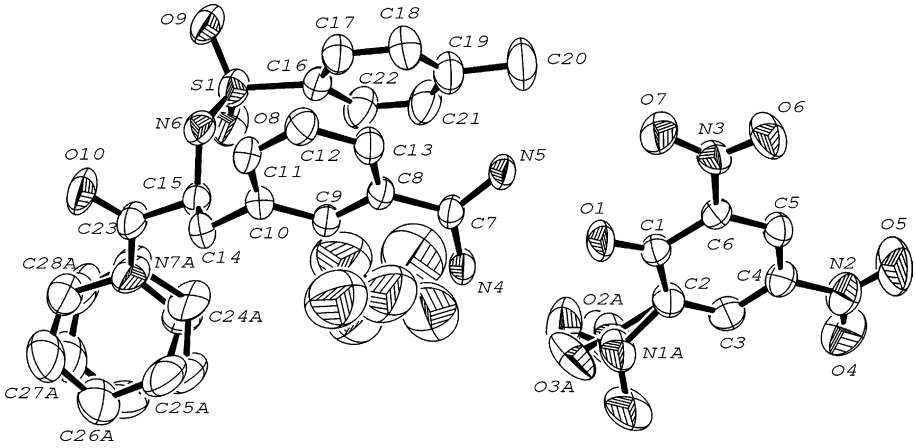

Figure 1. Asymmetric unit of the unit cell of 3-TAPAP picrate together with atom numbering. Hydrogen atoms were omitted for clarity. Only one (A) of two disordered piperidine rings and one of two disordered *nitro*-groups are labeled. Atomic displacement ellipsoids are drawn with 40% probability.

tween the amidine and benzene planes of 19.60° in 3-TAPAP is smaller than in the mentioned structures of benzamidine and benzdiamidine, where the corresponding angles are 27.71° and 24.52°, respectively.

The piperidine ring is clearly confined to one of two possible chair conformations. The displacement parameters of this group indicate its possible disorder, so this ring was refined in two positions resulting in an occupation factor of 0.5.

The conformation of picrate is comparable with those observed in other known structures. The *ortho*-NO_2 groups are not coplanar with the benzene ring. One of them (N1, O2, and O3) has significant atom displacement parameters, indicating its possible disorder and this group was refined in two positions resulting in occupation factors of 0.7 and 0.3. The torsion angles C1-C2-N1A-O2A, C1-C2-N1B-O2B, and C1-C6-N3-O7 are −41.5(2)°, 74(4)°, and −15.6(7)°, respectively. The bond angles C1-C2-C3 and C1-C6-C5 are much larger than 120°, their values being 125.7(4)° and 123.4°, respectively, while the bond angle C2-C1-C6 was found to decrease to the value of 111.4(4)°. These observations are in agreement with the correlations, which Szumna et al.[39] found for the picrate ion in structures retrieved from the Cambridge Structural Database. According to these authors, the deviation from planarity of the *ortho*-nitro groups is a consequence of repulsion between the phenolate and nitro oxygen atoms, and the simultaneous attraction of a partially positively charged nitrogen atom.

3-TAPAP picrate crystallizes with two water molecules which are disordered and their oxygen atoms were refined in seven positions with site occupation factors in the range between 0.2 and 0.4.

The packing of the molecules in the unit cell can be characterized by intermolecular interactions listed in Table 3 and shown in Figure 2A. The hydrogen atoms, H4A and H5A, of the nitrogens N4 and N5 of the amidine group are engaged in two kinds of intermolecular hydrogen bonds. Both protons are donated to the oxygen, O1, of the phenolate leading to formation of the canonical salt bridge. H4A and H5A are additionally shared by the oxygen atoms of the *ortho*-nitro groups, that is, by O3 (disordered) and O7, respectively. Thus, the hydrogen bonds, in which H4A and H5A take part, may be treated as bifurcated. The other hydrogen atoms, H4B and H5B of the amidine group, are donated, respectively, to the oxygen atoms, O9 of the sulfonyl group and to

Table 3. The hydrogen bond parameters

D–H	d(D–H) (Å)	d(H..A) (Å)	<DHA (°)	d(D..A) (Å)	A	Symmetry codes
N5–H5B	0.824	2.042	165.76	2.848(6)	O10	$-x, y-1/2, -z+1/2$
N5–H5A	0.800	2.019	147.71	2.729(5)	O1	
N5–H5A	0.800	2.518	139.01	3.166(6)	O7	
N4–H4A	0.860	2.091	143.03	2.826(5)	O1	
N4–H4A	0.860	2.519	145.76	3.266(13)	O3A	
N4–H4A	0.860	2.609	141.16	3.32(4)	O3B	
N4–H4B	0.860	2.172	163.34	3.006(5)	O9	$x-1/2, -y, z$
N6–H6	0.860	2.214	163.54	3.048(5)	O7	$-x, y+1/2, -z+1/2$

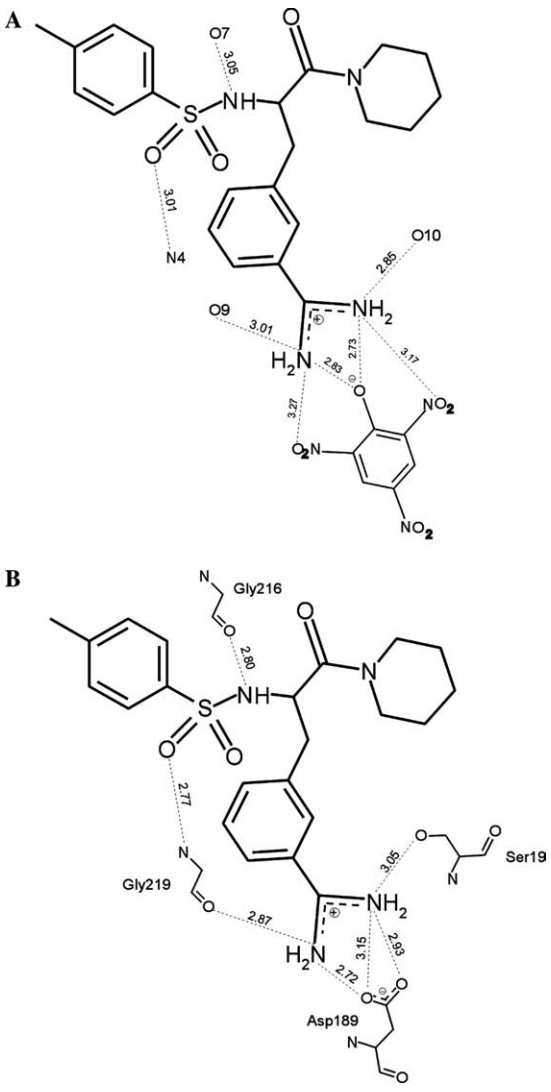

Figure 2. Patterns of hydrogen bonds formed by 3-TAPAP molecule in the structures of: (A) picrate, (B) βc-uPA complex. The hydrogen bonds are shown with broken lines with the distances of the interacting atoms given in Å.

O10 of the carbonyl group of another molecule. The nitrogen atom, N6, forms also an intermolecular hydrogen bond with O7 of the *ortho*-nitro group.

The arrangement of the molecules in the unit cell is dominated by the intermolecular hydrogen bonds, but it is also stabilized by stacking interaction between picrate ions (Fig. 3). An interesting feature is a system of channels parallel to x axis containing disordered clusters of water molecules.

The βc-uPA–3-TAPAP complex. The complex of βc-uPA with 3-TAPAP has been obtained in the crystal by the exchange of benzamidine. When we calculated difference electron density maps from data sets taken with 3-TAPAP soaked crystals, the inhibitor was clearly visible (see Fig. 5).

βc-uPA is a spherical molecule consisting of two opposed six-stranded β-barrels (Fig. 4), similar to other trypsin-like catalytic domains of serine proteinases.

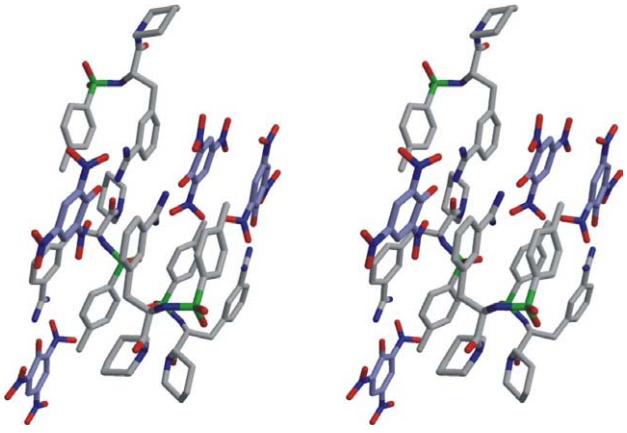

Figure 3. Stereo view of four 3-TAPAP picrate molecules showing their mutual packing. The disordered piperidine and nitro groups are not shown.

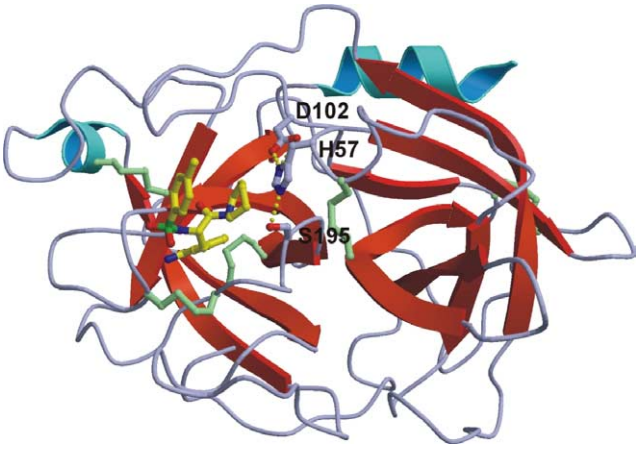

Figure 4. Ribbon representation of βc-uPA in complex with 3-TAPAP (yellow).

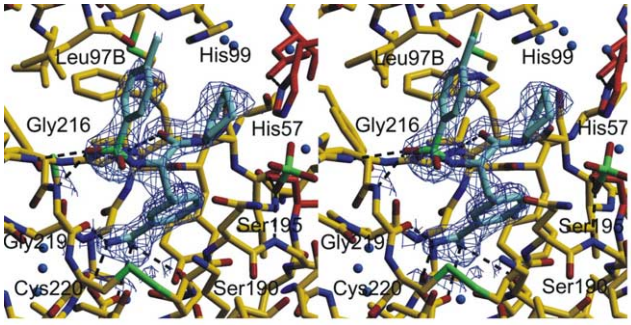

Figure 5. Stereo view of 3-TAPAP (blue) in the active site of βc-uPA (yellow). The Fo-Fc map contoured at 1σ around the inhibitor and calculated after extensive annealing of the structure with the inhibitor omitted is shown. The hydrogen bonds are shown with dashed black lines.

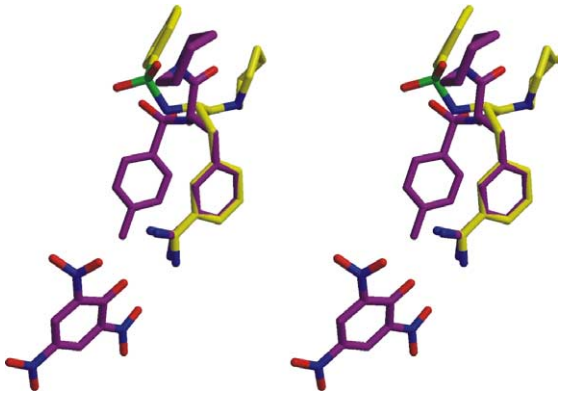

Figure 6. 3-TAPAP molecules in picrate (pick) and in the βc-uPA complex (yellow) with their benzene rings of benzamidine group overlapped. The disordered atoms are not shown.

The inhibitor fills the active site that is located at the junction between both barrels of the catalytic domain of βc-uPA, with only a few hydrogen bonds to the protein (Fig. 5).

The benzamidine group binds to the S1 specificity pocket and forms the canonical salt bridge with the carboxylate of Asp189, as well as hydrogen bonds with the carbonyl oxygen of Gly219 and O_γ of Ser190. The oxygen atom of the sulfonyl group forms a hydrogen bond with the nitrogen atom of Gly219, and the neighboring nitrogen atom, N6, forms a hydrogen bond with the oxygen atom of Gly216. The described hydrogen bonds together with the donor–acceptor distances are shown in Figure 2B. The piperidine ring is placed between the toluene and the imidazole ring of His57. The oxyanion hole is occupied by a sulfate anion from the solvent.

Comparison of 3-TAPAP conformation in different structures. The binding mode of 3-TAPAP in complex with uPA is similar to that of the 3-TAPAP in complex with trypsin.[27] 3-TAPAP is a 45-fold better inhibitor of trypsin (K_i = 1.2 μM) in comparison to uPA (K_i = 55 μM), and a 100-fold better inhibitor in comparison to tPA (K_i = 120 μM). The oxygen atom of the carbonyl group of 3-TAPAP in complex with trypsin forms a hydrogen bond with the nitrogen atom of Gly216, which we do not observe in the complex with uPA. In our structure, the inhibitor is further apart from the polypeptide chain and the carbonyl group has another orientation. This distance is in accordance with the presence of His99 in the structure of uPA instead of Leu99, which occurs in the structure of trypsin. Consequencely, the piperidine ring of the inhibitor has less room in the S2 pocket. On the basis of these observations, we can postulate that the lack of hydrogen bond between the carbonyl group of the inhibitor and peptide chain of protein is responsible for the weaker binding of 3-TAPAP to uPA in comparison to trypsin. uPA as well as trypsin have Ser190, but tPA has Ala190 instead of this amino acid residue. The hydroxyl group of Ser190 forms the hydrogen bonds with the inhibitor in uPA which is not possible in tPA. Therefore, the still weaker binding of 3-TAPAP to tPA seems to be caused by the lack of the hydrogen bond between Ala190 and the inhibitor.

The conformation of 3-TAPAP in the complex with βc-uPA has been compared to its conformation in 3-TAPAP picrate, which is shown in Figure 6. In this figure, the molecules are overlaid with their benzamidine groups positioned in the same plane. The distance between the asymmetric carbon atoms is 0.6 Å.

The orientation of the toluene and piperidine groups differs from each other. The toluene group in the picrate has hydrophobic contact with the benzamidine group, the distances between atoms of both groups being 3.6–4.3 Å. Similar orientation of the toluene group in the complex with protein is impossible, because in its place there is a polypeptide chain (amino acids 214–216). This difference leads to another orientation of the piperidine group. In the molecule of 3-TAPAP, there is freedom to rotate around the bonds C14-C15, C15-N6, and C15-C23, which enables the change of the conformation of the inhibitor, so that the binding to protein is more effective.

Comparison of the hydrogen-bonding patterns in the structure of 3-TAPAP picrate and in the structure of 3-TAPAP in its complex with uPA (Fig. 2) shows that in both structures the same inhibitor atoms are involved in a similar way in the formation of the intermolecular hydrogen bonds.

By the inspection of crystal structures of TAPA derivatives it became obvious that these inhibitors display high potency despite a relatively small number of polar interactions with the protein binding partners and overall small hydrophobic interaction surface. This controversy could be explained by the hydrophobic collapse of these inhibitors in solution in a way that the conformation finally recognized by the enzyme is preformed in solution. Collapsed structures, which would enhance the energy gain upon binding because entropically the conformational freedom is already reduced, were claimed by Ranatus et al.[40] for TAPAP-like molecules. These authors postulated folding of the inhibitor molecules in solution around their hydrophobic cores, i.e., hydrophobic collapse of the N- and C-terminal groups. Theoretical considerations of such

possibility were carried out by Lamb et al.[41] for a 3-TAPAP-similar compound, which is an inhibitor of FK506 binding protein. Simulation of this molecule conformational behavior in its unbound state in solution and in its bound state in the complex with the protein showed that the overall shapes of the inhibitor in both situations are comparable. According to the model obtained by Lamb et al., the aromatic ring and two aliphatic rings (one of them containing nitrogen atom) of this inhibitor had similar mutual orientations in solution and at the protein active site, the latter confirmed by crystal structure determination. Since, as far as the authors know, any studies of 3-TAPAP conformation in solution have not been performed, the question if it resembles the one in uPA–3-TAPAP complex cannot be directly answered. On the other hand, according to calculations with several optimization algorithms,[42] the global minimum conformation of 3-TAPAP was found to be relatively far (approximately 4.2 Å) from that determined in the crystal structure of its complex with trypsin.[27] In this connection, the shape of 3-TAPAP molecule observed in its crystalline complex with picrate showed that there exists at least one convincing conformation in an alternative hydrophobic collapse, in which the aromatic benzamidine moiety interacts with the toluene group and not with the aliphatic piperidine group.

Acknowledgments

We thank Professor Dr. Robert Huber for making it possible to determine the structure of 3-TAPAP in complex with uPA in his laboratory in Max-Planck-Institute in Martinsried, Germany. The authors are grateful to Dr. hab. Katarzyna Stadnicka and Mr. Jan Śliwiński from the Faculty of Chemistry, Jagiellonian University in Kraków (Poland), for their help in diffractometric measurement of 3-TAPAP picrate.

References and notes

1. Dudek, G. A.; Kloczewiak, M.; Budzynski, A. Z.; Latallo, Z. S.; Kopec, M. Characterisation and comparison of macromolecular end products of fibrinogen and fibrin proteolysis by plasmin. *Biochim. Biophys. Acta* **1970**, *214*, 44.
2. Liotta, L. A.; Goldfarb, R. H.; Brundage, R.; Siegal, G. P.; Terranova, V.; Garbisa, S. Effect of plasminogen activator (urokinase), plasmin, and thrombin on glycoprotein and collagenous components of basement membrane. *Cancer Res.* **1981**, *41*, 4629.
3. Chain, D.; Kreizman, T.; Shapira, H.; Shaltiel, S. Plasmin cleavage of vitronectin. Identification of the site and consequent attenuation in binding plasminogen activator inhibitor-1. *FEBS Lett.* **1991**, *285*, 251.
4. Mochan, E.; Keler, T. Plasmin degradation of cartilage proteoglycan. *Biochim. Biophys. Acta* **1984**, *800*, 312.
5. Vassalli, J. D.; Sappino, A. P.; Belin, D. The plasminogen activator/plasmin system. *J. Clin. Invest.* **1991**, *88*, 1067.
6. Chapman, H. A. Plasminogen activators, integrins, and the coordinated regulation of cell adhesion and migration. *Curr. Opin. Cell Biol.* **1997**, *9*, 714.
7. Lottenberg, R. A novel approach to explore the role of plasminogen in bacterial pathogenesis. *Trends Microbiol.* **1997**, *5*, 466, discussion 468.
8. Mayer, M. Biochemical and biological aspects of the plasminogen activation system. *Clin. Biochem.* **1990**, *23*, 197.
9. Lijnen, H. R.; Collen, D. Interaction of plasminogen activators and inhibitors with plasminogen and fibrin. *Semin. Thromb. Hemost.* **1982**, *8*, 2.
10. Rabbani, S. A; Xing, R. H. M. Role of urokinase (uPA) and its receptor (uPAR) in invasion and metastasis of hormone-dependent malignancies. *Int. J. Oncol.* **1998**, *12*, 911.
11. Irigoyen, J. P.; Munoz-Canoves, P.; Montero, L.; Koziczak, M.; Nagamine, Y. The plasminogen activator system: biology and regulation. *Cell Mol. Life Sci.* **1999**, *56*, 104.
12. Sidenius, N.; Blasi, F. The urokinase plasminogen activator system in cancer: recent advances and implication for prognosis and therapy. *Cancer Metast. Rev.* **2003**, *22*, 205.
13. Kook, Y. H.; Adamski, J.; Zelent, A.; Ossowski, L. The effect of antisense inhibition of urokinase receptor in human squamous cell carcinoma on malignancy. *EMBO J.* **1994**, *13*, 3983.
14. Crowley, C. W.; Cohen, R. L.; Lucas, B. K.; Liu, G.; Shuman, M. A.; Levinson, A. D. Prevention of metastasis by inhibition of the urokinase receptor. *Proc. Natl. Acad. Sci. USA* **1993**, *90*, 5021.
15. Fazioli, F.; Blasi, F. Urokinase-type plasminogen activator and its receptor: new targets for anti-metastatic therapy? *Trends Pharmacol. Sci.* **1994**, *15*, 25.
16. Ossowski, L.; Russo-Payne, H.; Wilson, E. L. Inhibition of urokinase-type plasminogen activator by antibodies: the effect on dissemination of a human tumor in the nude mouse. *Cancer Res.* **1991**, *51*, 274.
17. Wilhelm, O.; Schmitt, M.; Hohl, S.; Senekowitsch, R.; Graeff, H. Antisense inhibition of urokinase reduces spread of human ovarian cancer in mice. *Clin. Exp. Metast.* **1995**, *13*, 296.
18. Magdolen, V.; Rettenberger, P.; Koppitz, M.; Goretzki, L.; Kessler, H.; Weidle, U. H.; Konig, B.; Graeff, H.; Schmitt, M.; Wilhelm, O. Systematic mutational analysis of the receptor-binding region of the human urokinase-type plasminogen activator. *Eur. J. Biochem.* **1996**, *237*, 743.
19. Burgle, M.; Koppitz, M.; Riemer, C.; Kessler, H.; Konig, B.; Weidle, U. H.; Kellermann, J.; Lottspeich, F.; Graeff, H.; Schmitt, M.; Goretzki, L.; Reuning, U.; Wilhelm, O.; Magdolen, V. Inhibition of the interaction of urokinase-type plasminogen activator (uPA) with its receptor (uPAR) by synthetic peptides. *Biol. Chem.* **1997**, *378*, 231.
20. Jankun, J.; Keck, R. W.; Skrzypczak-Jankun, E.; Swiercz, R. Inhibitors of urokinase reduce size of prostate cancer xenografts in severe combined immunodeficient mice [published erratum appears in Cancer Res 1998 Jan 1;58(1):179]. *Cancer Res.* **1997**, *57*, 559.
21. Alonso, D.; Tejera, A. M.; Farias, E. F.; Bal de Kier Joffe, E.; Gomez, D. E. Inhibition of mammary tumor cell adhesion, migration, and invasion by the selective synthetic urokinase inhibitor B428. *Anticancer Res.* **1998**, *18*, 4499.
22. Zeslawska, E.; Schweinitz, A.; Karcher, A.; Sondermann, P.; Sperl, S.; Sturzebecher, J.; Jacob, U. Crystals of the urokinase type plasminogen activator variant beta c-uPA in complex with small molecule inhibitors open the way towards structure-based drug design. *J. Mol. Biol.* **2000**, *301*, 465.
23. Nienaber, V. L.; Davidson, D.; Edalji, R.; Giranda, V. L.; Klinghofer, V.; Henkin, J.; Magdalinos, P.; Mantei, R.; Merrick, S.; Severin, J. M.; Smith, R. A.; Stewart, K.;

Walter, K.; Wang, J. Y.; Wendt, M.; Weitzberg, M.; Zhao, X. M.; Rockway, T. Structure-directed discovery of potent non-peptidic inhibitors of human urokinase that access a novel binding subsite. *Struct. Fold Des.* **2000**, *8*, 553.
24. Katz, B. A.; Mackman, R.; Luong, Ch.; Radika, K.; Martelli, A.; Sprengeler, P. A.; Wang, J.; Chan, H.; Wong, L. Structural basis for selectivity of small molecule, S1-binding, submicromolar inhibitor of urokinase-type plasminogen activator. *Chem. Biol.* **2000**, *4*, 299.
25. Katz, B. A.; Elrod, K.; Luong, C.; Rice, M. J.; Mackman, R. L.; Sprengeler, P. A.; Spencer, J. H.; Janc, J.; Link, J.; Litvak, J.; Rai, R.; Rice, K.; Sideris, S.; Verner, E.; Young, W. A novel serine protease inhibition motif involving a multi-centered short hydrogen bonding network at the active site. *J. Mol. Biol.* **2001**, *307*, 1451.
26. Zeslawska, E.; Jacob, U.; Schweinitz, A.; Coombs, G.; Bode, W.; Madisom, E. Crystals of urokinase type plasminogen activator complexes reveal the binding mode of peptidomimetic inhibitors. *J. Mol. Biol.* **2003**, *328*, 109.
27. Turk, D.; Stürzebecher, J.; Bode, W. Geometry of binding of the *N*-alpha-tosylated piperidides of *m*-amidino-, *p*-amidino- and *p*-guanidino phenylalanine to thrombin and trypsin. X-ray crystal structures of their trypsin complexes and modeling of their thrombin complexes. *FEBS Lett.* **1991**, *287*, 133.
28. Wagner, G.; Horn, H.; Richter, P.; Vieweg, H.; Lischke, I.; Kazimirowski, H. G. Synthesis of antiproteolytically active *N*α-arylsulfonylated aminophenyl- alanine amides. *Pharmazie* **1981**, *36*, 597.
29. Otwinowski, Z.; Minor, W. Processing of X-ray diffraction data collected in oscillation mode. *Methods Enzymol.* **1997**, *276*, 307.
30. Sheldrick, G. M. Phase annealing in SHELX-90: direct methods for larger structures. *Acta Cryst. A* **1990**, *46*, 467.
31. Sheldrick, G. M. *SHELXL97*; University of Göttingen: Germany, 1997.
32. Farrugia, L. J. Ortep-3 for Windows—a version of ORTEP-III with a Graphical User Interface (GUI). *J. Appl. Cryst.* **1997**, *30*, 565.
33. Bailey, S. The CCP4 suite—programs for protein crystallography. *Acta Crystallogr. D* **1994**, *50*, 760.
34. Jones, T. A. A graphics model building and refinement system for macromolecules. *J. Appl. Cryst* **1978**, *11*, 268.
35. Brünger, A. T. Crystallography and NMR system—a new software suite for macromolecular structure determination. *Acta Cryst. D* **1998**, *54*, 905.
36. Engh, R. A.; Huber, R. Accurate bond and angle parameters for X-ray protein-structure refinement. *Acta Cryst. A* **1991**, *47*, 392.
37. Barker, J.; Phillips, P. R.; Wallbridge, M. G. H.; Powell, H. R. Benzamidine. *Acta Cryst. C* **1996**, *52*, 2617.
38. Jokic, M.; Bajic, M.; Zinic, M.; Peric, B.; Kojic-Prodic, B. Benzdiamidine. *Acta Cryst. C* **2001**, *57*, 1354.
39. Szumna, A.; Jurczak, J.; Urbańczyk-Lipkowska, Z. Competition between π–π stacking and hydrogen bonding in (1:2) picrates of 1,5-diamino-3-oxapentane, 1,8-diamino-3,6-dioxaoctane and 1,5-diamino-3-azapentane—solid state studies. *J. Mol. Struct.* **2000**, *526*, 165.
40. Renatus, M.; Bode, W.; Huber, R.; Stürzebecher, J.; Stubbs, M. T. Structural and functional analyses of benzamidine-based inhibitors in complex with trypsin: implications for the inhibition of factor Xa, tPA and urokinase. *J. Med. Chem.* **1998**, *41*, 5445.
41. Lamb, M. L.; Tirado-Rives, J.; Jorgensen, W. L. Estimation of the binding affinities of FKBP12 inhibitors using a linear response method. *Bioorg. Med. Chem.* **1999**, *7*, 851.
42. Diller, D. J.; Verlinde, L. M. J. A critical evaluation of several global optimization algorithms for the purpose of molecular docking. *J. Comput. Chem.* **1999**, *20*, 1740.